9. A. J. Groszek, *Nature* **196**, 531 (1962); *ibid.* **204**, 680 (1964); *Proc. R. Soc. London Ser. A* **314**, 473 (1970).
10. G. H. Findenegg and M. Lippard, *Carbon* **25**, 119 (1987).
11. G. D. Parfitt and E. Willis, *J. Phys. Chem.* **68**, 1780 (1964).
12. P. H. Lippel, R. J. Wilson, M. D. Miller, Ch. Wöll, S. Chiang, *Phys. Rev. Lett.* **62**, 171 (1989).
13. J. K. Spong *et al.*, *Nature* **338**, 137 (1989).
14. D. P. E. Smith, J. K. H. Hörber, G. Binnig, H. Nejoh, *ibid.* **344**, 641 (1990).
15. W. Mizutani, M. Shigeno, M. Ono, K. Kajimura, *Appl. Phys. Lett.* **56**, 1974 (1990).
16. H. Ohtani, R. J. Wilson, S. Chiang, C. M. Mate, *Phys. Rev. Lett.* **60**, 2398 (1988).
17. R. Lazzaroni, A. Calderone, G. Lambin, J. P. Rabe, J. L. Brédas, *Synth. Metals* **41**, 525 (1991).
18. J. P. Rabe, M. Sano, D. Batchelder, A. A. Kalatchev, *J. Microsc. (Oxford)* **152**, 573 (1988).
19. S. Buchholz and J. P. Rabe, *J. Vac. Sci. Technol. B*, in press.
20. G. C. McGonigal, R. H. Bernhardt, D. J. Thomson, *Appl. Phys. Lett.* **57**, 1 (1990).
21. A. I. Kitaigorodskij and J. B. Mnjukh, *Bull. Acad. Sci. U.S.S.R. Div. Chem. Sci.* (1959), p. 1992.
22. This project was supported by the Bundesministerium für Forschung und Technologie under the title "Ultrathin Polymer Layers" 03M4008E9 and the European Science Foundation (Additional Activity: Chemistry and Physics of Polymer Surfaces and Interfaces). S.B. acknowledges support through a Kekulé scholarship, granted by the Verband der Chemischen Industrie.

11 March 1991; accepted 29 May 1991

Dislocations and Flux Pinning in $YBa_2Cu_3O_{7-\delta}$

S. JIN, G. W. KAMMLOTT, S. NAKAHARA, T. H. TIEFEL, J. E. GRAEBNER

Bulk $YBa_2Cu_3O_{7-\delta}$ superconductors, under certain processing conditions such as melt texturing, exhibit a very high dislocation density of 10^9 to 10^{10} per square centimeter. In addition, the density of low-angle grain boundaries in such samples can be significantly increased (to less than ~700-nanometer spacing) through a dispersion of submicrometer-sized Y_2BaCuO_5 inclusions. These defect densities are comparable to those in high critical current thin films as revealed through scanning tunneling microscopy, and yet the critical current densities in the bulk materials (at 77 kelvin and a field of 1 tesla for example) remain at a 10^4 amperes per square centimeter level, about two orders of magnitude lower than in thin films. The results imply that these defect density levels are not significant enough to explain the difference in flux pinning strength between the thin film and bulk materials. The observation of spiral-like growth of the superconductor phase in bulk Y-Ba-Cu-O is also reported.

THE MAIN ADVANTAGE OF A SUPERconductor over a conventional conductor such as copper is the large amount of electrical current that it can carry by virtue of its zero resistance. Thus high current-carrying capability is essential for major bulk applications of the new, high transition temperature (T_c) superconductors. Epitaxial thin films of the high T_c superconductor $YBa_2Cu_3O_{7-\delta}$ typically exhibit high critical current densities (J_c) in excess of 10^6 A cm^{-2} at 77 K even in the presence of strong magnetic fields. The bulk materials, on the other hand, have about two orders of magnitude lower J_c (~10^4 A cm^{-2}).

Hawley *et al.* (*1*) and Gerber *et al.* (*2*) have recently observed, through scanning tunneling microscopy, a high density of screw dislocations (~10^9 cm^{-2}) associated with spiral growth in epitaxial thin films of Y-Ba-Cu-O. They discuss the possibility of flux pinning by the observed screw dislocations (and the defects in low angle grain boundaries between the spirals), and suggest that the high dislocation density may be related to the significantly higher J_c in thin films than in bulk materials. We report here the observation of a comparably high density of dislocations in some bulk Y-Ba-Cu-O superconductors and discuss the possible relationship of the defects to the flux pinning behavior in bulk and thin film superconductors.

Bulk $YBa_2Cu_3O_{7-\delta}$ samples ("123" phase) were prepared in three different forms; sintered pellets (940°C for 40 hours in O_2 and furnace cool), sintered ribbons (~6-μm-thick $YBa_2Cu_3O_{7-\delta}$ on ~12-μm-thick silver substrate by spray coating of powder, cold rolling by ~90% reduction in cross-sectional area, and sintering at 940°C for 100 hours in O_2 and furnace cool), and locally melt-textured bars (continuous cooling, in the absence of temperature gradient, from ~1050° to 380°C at 2° to 10°C per hour in O_2).

The dispersion of fine Y_2BaCuO_5 inclusions ("211" phase) was made by melt-texture processing of off-stoichiometric samples containing a fine-scale compositional segregation richer in Y and Ba (*3*, *4*). The resultant samples contained about 30 to 45 vol. % of submicrometer-sized "211" particles in "123" matrix. All the samples exhibited T_c ($R = 0$) > 90 K and T_c (midpoint) by ac susceptibility measurement of 90 to 95K.

Transmission electron microscopy (TEM) for the analysis of dislocations in Y-Ba-Cu-O (*5*) was carried out using a Philips 430 electron microscope operated at 300 kV. Scanning electron microscopy (SEM) was conducted at 20 kV. Magnetization measurements (*M-H* hysteresis loops) were made at 77 K with a vibrating sample magnetometer using a sweep rate of ~80 Oe s^{-1} and the maximum applied field of ±9 T. The intragranular J_c (which is proportional to flux pinning strength) was estimated from the *M-H* loop by using the Bean model (*6*). The average grain diameter based on high-angle boundaries was used as the size of the supercurrent loop, as it is well established that low-angle grain boundaries in Y-Ba-Cu-O are not weak links.

The TEM micrograph for the melt-textured sample (Fig. 1) shows an example of a high density of dislocations estimated to be in excess of 10^9 cm^{-2}. This is in sharp contrast to the sintered samples which typically contain relatively few dislocations (10^6 to 10^7 cm^{-2}). The exact cause for the increased number of dislocations in melt-textured Y-Ba-Cu-O is not clearly understood, but it may be related to a number of factors such as (i) the accommodation, during crystal growth below 1000°C, of lattice parameter changes in the presence of local cation concentration gradient, (ii) the relief of internal stresses caused by local temperature gradient, (iii) the strains associated with the merger of parallel "123" plates with slight misorientations, (iv) the strains caused by bending and forced merger of neighboring "123" plates as the trapped $BaCuO_2$ or CuO phase between them is removed by diffusion or evaporation (a 10 to 30% decrease in weight is common in melt-texture processing owing to the partial loss of BaO and

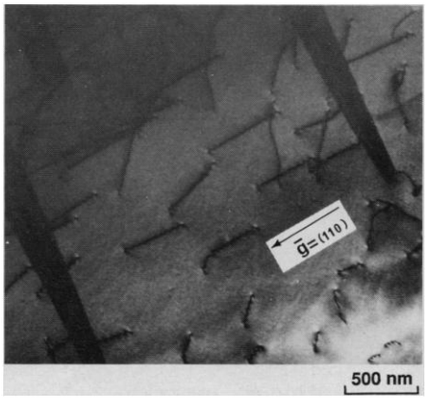

Fig. 1. TEM micrograph showing dislocations in melt-textured Y-Ba-Cu-O.

AT&T Bell Laboratories, Murray Hill, NJ 07974.

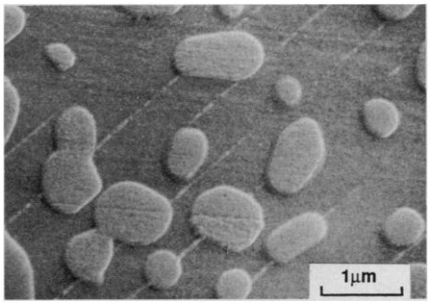

Fig. 2. SEM microstructure of a melt-textured sample containing submicrometer-sized "211" inclusions. The low-angle grain boundaries are seen as parallel lines.

CuO by evaporation or liquid dripping down), and (v) the thermal contraction mismatch between the "123" matrix and the "211" inclusions. None of these factors are applicable to the case of sintered materials. The dislocations in the melt-textured samples are edge-, screw-, or mixed-type with [100] or [010] Burgers vectors. The slip occurs on all three orthogonal planes of (010), (100), or (001), as reported previously (*5*).

The melt-textured samples also contain a large number of plate boundaries (presumably low-angle grain boundaries) present between the neighboring "123" plates. The spacing between these boundaries is typically about 5000 nm; however, it can be even further reduced if a dispersion of finer "211" particles is made (Fig. 2). The density of the boundaries is significantly increased as the spacing between them is reduced now to ~700 nm. The presence of the "211" inclusions (~800 nm average diameter, ~35 vol. %) apparently increases the nucleation of "123" plates during crystallization and retards the coarsening process during slow cooling.

Shown in Table 1 are the dislocation density, the average spacing of plate boundaries, and the intragranular J_c at 77 K, H = 1 T. As is evident from the table, the increase in dislocation density from $< 10^7$ to 10^9 to 10^{10} cm^{-2} does not noticeably influence the critical current density (and flux pinning). Increasing the density of plate boundaries (low-angle grain boundaries) also seems to have little beneficial effect on J_c. [The possible effect of small "211" inclusions on flux pinning has been discussed in previous publications (*3, 7*)].

The dislocation density in melt-textured Y-Ba-Cu-O given in Table 1 (10^9 to 10^{10} cm^{-2}) is comparable to the values reported by Hawley *et al.* (*1*) and Gerber *et al.* (*2*) for high-J_c thin films (~10^9 cm^{-2}), and yet the $J_c(H)$ values in the bulk material remain at ~10^4 A cm^{-2}, about two orders of magnitude lower than in thin films, even in the low field regime where the vortex spacing may be comparable to the dislocation spacing.

Hawley *et al.* (*1*) also suggest that the large number of low-angle grain boundaries (and associated defects) which would form as the spiral grains meet each other may serve as flux pinning sites. The size of the spirals (that is, the spacing between the low-angle grain boundaries) in their paper is about 300 to 900 nm, which is comparable to the value for the melt-textured sample with "211" dispersions (~700 nm). The spiral size (as well as the density of [001] or near [001] screw dislocations) in their thin films also appears to be in the same order of magnitude as that in our ribbon samples as will be discussed later. Both the melt-textured sample and the ribbons exhibit J_c values two orders of magnitude less than the films examined by Hawley *et al.* (*1*).

The pinning efficiency of dislocations and low-angle grain boundaries may vary depending on their geometry and the relative orientations and spacings between the vortex lines and the pinning defects. In *c*-axis–oriented films, the screw dislocations lie along [001]. If the applied field is parallel to [001], the dislocations can capture fluxoid cores efficiently and their pinning effect would be expected to be much larger in thin films than in bulk materials where a significant portion of the total dislocations is not parallel to the fluxoid. In the case of textured ribbons (Fig. 3B), however, there may be many, favorably oriented (parallel to [001]) dislocations associated with the growth spirals. The actual J_c measurements on epitaxial Y-Ba-Cu-O thin films showed some anisotropy in critical current density (*8*) (higher J_c values when the applied field was aligned along the *a-b* plane rather than along the [001] direction). The anisotropy factor was small; only about 2 at 77 K. The dislocation spacings as well as the low-angle-boundary spacings in both the thin films and the melt-textured bulk samples appear to be far greater than the vortex spacing in high magnetic fields ($H \geq 1$ T), making it difficult to account for the high degree of flux pinning.

The growth spirals of the $YBa_2Cu_3O_{7-\delta}$ phase observed during epitaxial film deposition (*1, 2*) are an interesting feature which may provide an insight into the growth mechanism. We have recently observed a

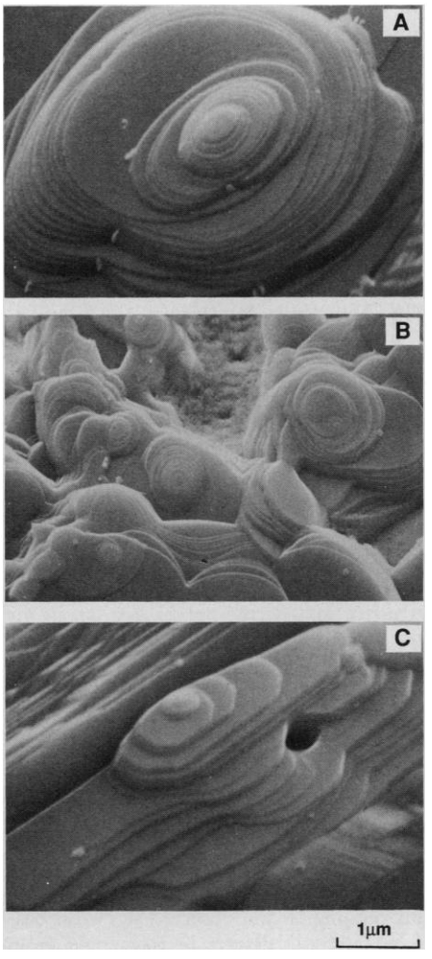

Fig. 3. SEM photograph showing (**A**) a spiral-like growth on the surface of Y-Ba-Cu-O ribbons (notice the local blockage of layer expansion near small inclusions), (**B**) from another region of the ribbon sample, and (**C**) an area with a coarsened structure.

Table 1. Dislocation density and J_c in bulk Y-Ba-Cu-O.

Material	Dislocation density (cm^{-2})	Plate boundary spacing (nm)	Intragranular J_c (77 K, H = 1 T) (10^4 A cm^{-2})
Sintered pellet	$<10^7$	Few present	1.6
Ribbon			1.2
Melt-textured bar*	10^9 to 10^{10}	5000	1.3
Melt-textured bar (off-stoichiometric)†		700	1.4

*Contains ~14 vol. % of ~9000-nm size "211" inclusions. †Contains ~35 vol. % of ~800-nm size "211" inclusions.

related, spiral-like growth pattern on the surfaces of bulk $YBa_2Cu_3O_{7-\delta}$ ribbons (and occasionally on sintered pellets). Shown in Fig. 3 are scanning electron microscopy photographs from the surface of the ribbon sample. The appearance of spiral-like growth is evident in the figures, although the actual spirals are not as clearly defined and the step heights are much coarser (estimated to be about 10 to 100 nm within the resolution of the scanning electron microscope) than the unit-cell-high steps revealed by scanning tunneling microscopy (*1, 2*). These differences are attributed to the extensive coarsening of the structure in our samples after the long heat treatment of 940°C for 100 hours. The driving forces for the observed spiral-like growth may be the recrystallization and coarsening of severely strained and finely pulverized/smeared $YBa_2Cu_3O_{7-\delta}$ phase (caused by heavy cold rolling of the ribbons). The flat surface on each layer is believed to be the *a-b* plane along which the growth is known to be rapid.

The results in the present investigation imply that the dislocation density levels of 10^9 to 10^{10} cm^{-2} are not sufficient to explain the large difference in critical current densities between thin film and bulk Y-Ba-Cu-O. However, the dislocations remain as appealing pinning centers, as their core dimension is comparable to the coherence lengths in high T_c cuprate superconductors. Knowing that the density of dislocations can be significantly increased through materials synthesis and processing, as demonstrated by Hawley *et al.* (*1*) and Gerber *et al.* (*2*) as well as the present work, one of the possible approaches for significant pinning enhancement in high T_c superconductors may be to find practical techniques for increasing the density further by at least a few orders of magnitude.

REFERENCES

1. M. Hawley, I. D. Raistrick, J. G. Berry, R. J. Houlton, *Science* **251**, 1587 (1991).
2. C. Gerber, D. Anselmetti, J. G. Bednorz, J. Mannhart, D. G. Schlom, *Nature* **350**, 279 (1991).
3. S. Jin, T. H. Tiefel, G. W. Kammlott, *Appl. Phys. Lett.* **59**, 540 (1991).
4. S. Jin *et al.*, unpublished.
5. S. Nakahara, S. Jin, R. C. Sherwood, T. H. Tiefel, *Appl. Phys. Lett.* **54**, 1926 (1989).
6. C. P. Bean, *Rev. Mod. Phys.* **36**, 31 (1964).
7. M. Murakami *et al.*, *Cryogenics* **30**, 390 (1990).
8. B. Roas, L. Schultz, G. Saemann-Ischenko, *Phys. Rev. Lett.* **64**, 479 (1990).

14 May 1991; accepted 20 June 1991

Order and Disorder in C_{60} and K_xC_{60} Multilayers: Direct Imaging with Scanning Tunneling Microscopy

Y. Z. Li, M. Chander, J. C. Patrin, J. H. Weaver, L. P. F. Chibante, R. E. Smalley

Monolayer and multilayer structures of C_{60}, a high temperature van der Waals solid, have been studied with scanning tunneling microscopy. Structures grown on GaAs(110) at 300 kelvin and at elevated temperatures show significantly different morphologies because of balances between thermodynamics and kinetics. Condensation onto stepped surfaces demonstrates preferred bonding and nucleation at step edges. Detailed studies of potassium incorporation in crystalline C_{60} show highly ordered structures in the K_3C_{60} metallic state but disordered non-metallic structures for high potassium concentrations.

Recent breakthroughs (*1*) in the synthesis of C_{60} and related fullerenes (*2*) have made possible studies of the electronic (*3–5*), electrical (*6–9*), and structural (*10–16*) properties of these novel forms of carbon in pure and compound form. Structural transformations for pure C_{60} from face-centered cubic (fcc) to simple cubic (sc) have been observed upon cooling (*13*), and an fcc-bcc (body-centered cubic) tranformation has been reported upon reaction to form K_6C_{60} (*14*). Mobile hexagonal arrays of mixed C_{60} and C_{70} have been observed on Au(111), where surface interaction was very weak (*10*). Scanning tunneling microscopy (STM) results for C_{60} growth on GaAs(110) at 300 K revealed large stable monolayer islands and distinct adsorption sites (*11*). Variations in molecular height relative to the surface were related to the structure of the relaxed GaAs(110) substrate. It was not known, however, whether the bonding sites represented an equilibrium structure or one dictated by kinetics, that is, a growth structure. Since the spherical C_{60} molecule is bound by van der Waals interaction and desorbs in ultrahigh vacuum at ~550°C, C_{60} monolayers, multilayers, and solids offer unique opportunities to explore crystal growth driven by a simple interaction potential. The discovery of alkali metal incorporation into the fullerene lattice (*6–9*) raised questions as to the structure of thin films in the conducting and superconducting phase where ionic interactions were introduced.

This paper focuses on thin film structures of pure and K-doped C_{60} grown on GaAs(110). With STM, we have examined C_{60} monolayers and multilayers prepared at temperatures from 300 K to 470 K. The results show that ordered C_{60} structures can be commensurate or incommensurate with the substrate. Multilayer growth at 300 K produces growth structures with point defects, dislocations, domain boundaries, and surface faceting. Multilayer C_{60} growth at 470 K yields structures that are almost per-

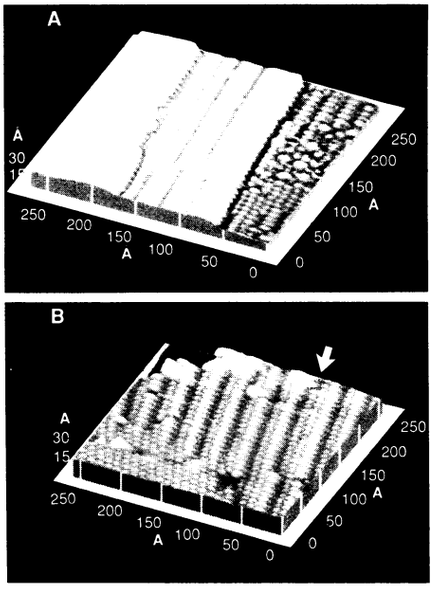

Fig. 1. STM images of kinetically limited C_{60} multilayer growth structures at 300 K. Image (**A**) reveals first, second, and third layers, while (**B**) focuses on an area of the third layer. Row-like structures in (A) run along the [$\bar{1}$11] direction of the substrate, and they expose mainly (311) and (211) faces of the fcc lattice in which the (111) terrace normals are not perpendicular to the surface. The sawtooth structure at the center of (B) consists of (211) and (533) faces, the latter indicated by an arrow. The lower left corner shows a (111) close-packed face.

Y. Z. Li, M. Chander, J. C. Patrin, J. H. Weaver, Department of Materials Science and Chemical Engineering, University of Minnesota, Minneapolis, MN 55455.
L. P. F. Chibante and R. E. Smalley, Rice Quantum Institute and Departments of Chemistry and Physics, Rice University, Houston, TX 77251.